An Integral-Equation Technique for Solving Thick Irises in Rectangular Waveguides

Ivica Stevanović, *Member, IEEE*, Pedro Crespo-Valero, and Juan R. Mosig, *Fellow, IEEE*

***Abstract*—This paper presents an efficient integral-equation (IE) technique for analysis of thick irises inside multilayered rectangular waveguides. The IEs remain the same as in the case of zero-thickness iris and the thickness is accounted for only as a correction term in the IE kernel. This technique halves the number of unknowns on the iris, thus leading to computational effort and simulation times comparable to the zero-thickness case. In this paper, two efficient ways for computing the correction term are introduced and the accuracy of the approach is discussed on several waveguide structures and filters.**

***Index Terms*—Green's functions, integral equations (IEs), multilayered structures, rectangular waveguide discontinuities, stratified media theory, thick irises.**

I. Introduction

A THICK iris, defined as an aperture in a metallic wall of finite thickness, is one of the most common types of discontinuities encountered in waveguides. These apertures can arise in the waveguide external walls (slot waveguide antennas, coupling holes between waveguides) or in additional walls filling the waveguide cross section and dividing the waveguide into coupled cavities, useful to create filtering structures. From this second point-of-view, irises were first analyzed in the early 1950s, by means of approximate analytical and variational techniques, well detailed in classical textbooks [1]–[4]. Initially, these approximate expressions were derived for small apertures in zero-thickness conducting walls, but correction factors for larger apertures and/or finite thickness walls [5]–[7] were soon introduced. The first systematic technique for the full-wave analysis of irises in waveguides was the mode-matching (MM) technique [8], [9]. Specific applications for several regular iris shapes can be found in [10]–[13]. Today, in order to cope with arbitrary shapes and more complicated geometries, so-called hybrid methods are used, where the MM is combined with integral-equation (IE) approaches [14] or with finite-element method (FEM) algorithms [15]–[17]. The excellent review paper by Arndt *et al.* [18] gives a comprehensive and up-to-date survey. In addition to these, there is another group of hybrid-analysis methods developed for planar discontinuities embedded within layered media inside waveguides: the generalized scattering matrix (GSM) procedure used in conjunction with the method of moments (MoM) [19], [20] or finite-difference time-domain (FDTD) method [21].

Manuscript received January 20, 2005; revised June 13, 2005.

The authors are with the Laboratory of Electromagnetics and Acoustics, Ecole Polytechnique Fédérale de Lausanne, CH-1015 Lausanne, Switzerland (e-mail: ivica.stevanovic@epfl.ch; pedro.crespovalero@epfl.ch; juan.mosig@epfl.ch).

Digital Object Identifier 10.1109/TMTT.2005.860305

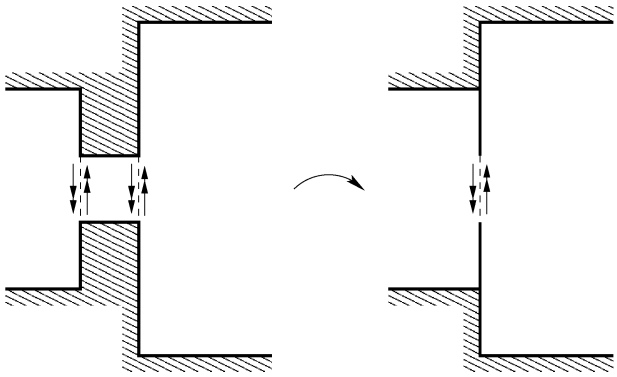

Fig. 1. Thick iris modeled as a zero-thickness iris.

In parallel to these developments, slots in waveguides have been also analyzed with classical IE approaches using the equivalence principle [22]. In this context, the problem of thick irises inside waveguides is equivalent to the problem of apertures of a finite thickness in printed multilayered antennas. Recently, an IE-based approximate model has shown that the apertures of finite thicknesses can be treated as infinitely thin (Fig. 1) with the thickness appearing only as a modification of the Green's functions. Theoretical developments for this approach [23] have now been experimentally validated [24].

In this paper, we first review the IE model for general waveguide discontinuities and we adapt it to our needs, especially in terms of excitation models and numerical algorithms. We then combine it with the approximate model for thick irises and apply it to several waveguide structures and filters to show the flexibility and potentialities of the combined formulation.

II. IEs and MoM

Consider a structure composed of a number of waveguides with different rectangular cross sections (Fig. 2). Any interconnection between waveguides of different cross sections and any zero-thickness iris is treated like a slot in the standard slot antenna formulation. An iris with a nonzero-thickness will be considered *ab initio* as a new waveguide cross section. However, for not very thick irises, an original and efficient treatment will be introduced later on. On the other hand, any waveguide section can by filled by stratified dielectrics and include conductive patches of arbitrary shapes localized in planes perpendicular to the propagation direction.

In the IE formulation of the problem, the boundary conditions for the fields are imposed. On every interconnection of two different waveguides and every slot, the surface equivalence principle is applied and magnetic surface currents $\mathbf{J}_H$ (on both sides

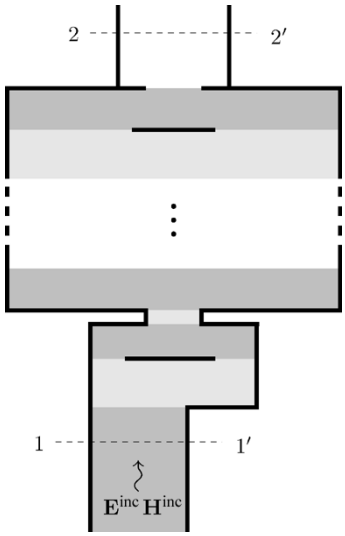

Fig. 2. General multilayered waveguide structure composed of an arbitrary number of planar printed patches and slots.

of the interface) are introduced in such a way as to insure the continuity of the tangential component of the total electric field

$$\mathbf{E}_{\tan}^{+} = \mathbf{E}_{\tan}^{-} \Leftrightarrow \mathbf{J}_{H}^{+} = -\mathbf{J}_{H}^{-}. \tag{1}$$

The continuity of tangential component of the total magnetic fields on the slots and the interconnections of two different waveguides has to be satisfied as follows:

$$\mathbf{H}_{\tan}^{+} = \mathbf{H}_{\tan}^{-}. \tag{2}$$

Every patch surface is modeled using electric surface currents $\mathbf{J}_E$. Considering all the patches to be made of perfectly conducting metallizations, the tangential component of the total electric field $(\mathbf{E})$ on them has to be set to zero as follows:

$$\mathbf{E}_{\tan} = \mathbf{E}_{\tan}^{\text{inc}} + \mathbf{E}_{\tan}^{\text{scatt}} = \mathbf{0} \tag{3}$$

where $\mathbf{E}^{\text{inc}}$ and $\mathbf{E}^{\text{scatt}}$ are the incident and scattered electric fields, respectively.

Introducing field Green's functions, the scattered fields can be expressed as convolution integrals of the electric and/or magnetic sources and the corresponding Green's functions. The boundary conditions evolve this way into a system of IEs with unknown electric and magnetic surface currents.

The MoM technique has been used for numerical solving of the system of IEs. The unknown electric and magnetic currents are expanded into a set of basis functions. In order to model the general shape of magnetic and electric planar sources, subsectional (rectangular/triangular) basis functions have been selected so the unknown sources can be expanded as follows:

$$\mathbf{J}_Q(\mathbf{r}') = \sum_k \alpha_{Qk}\mathbf{f}_{Qk}(\mathbf{r}'), \qquad k = 1, \ldots, N_Q \tag{4}$$

where the source index $Q = E$ for a horizontal electric dipole (HED) or $Q = H$ for a horizontal magnetic dipole (HMD). In the same expression, α_{Qk} are the unknown coefficients in the expansion of the currents and $\mathbf{f}_{Qk}$ are the N_Q subsectional basis functions defined on electric $(Q = E)$ or magnetic $(Q = H)$ surfaces.

Using the Galerkin procedure, the same set of functions as the one used for the basis functions is chosen. This way, the original coupled system of IEs is transformed into an algebraic linear system of equations with coefficients α_{Qk} as unknowns as follows:

$$\begin{bmatrix} [R_{EE}] & [R_{EH}] \\ [R_{HE}] & [R_{HH}] \end{bmatrix} \begin{bmatrix} [\alpha_E] \\ [\alpha_H] \end{bmatrix} = \begin{bmatrix} [\gamma_E] \\ [\gamma_H] \end{bmatrix}. \tag{5}$$

There are four different types of terms R_{PQ} that appear in the final MoM matrix. The term (k, l) in each submatrix can be written in a condensed form as

$$R_{PQ}(k,l) = \int_{S_k} \mathbf{f}_{Pk}(\mathbf{r})dS \int_{S_l} \overleftrightarrow{\mathbf{G}}_{PQ}(\mathbf{r}|\mathbf{r}')\mathbf{f}_{Ql}(\mathbf{r}')\,\mathrm{d}S'. \tag{6}$$

Using the equivalent transmission-line networks to represent the waveguide sections, the field dyadic Green's functions are given by

$$\overleftrightarrow{\mathbf{G}}_{PQ}(\mathbf{r}|\mathbf{r}') = \sum_i \widetilde{G}_{Pi}(z,z')\mathbf{p}_i(x,y)\mathbf{q}_i(x',y'). \tag{7}$$

It must be pointed out that the above is a compact notation where both the observer index P and the source index Q can be either E (electric field, electric source) or H (magnetic field, magnetic source). Accordingly, the vector mode functions $\mathbf{p}$ and $\mathbf{q}$ are either the modal function of electric $(\mathbf{e})$ or of magnetic $(\mathbf{h})$ type. Finally, $\widetilde{G}_{Pi}(z,z')$, depending only on the observer index, is the associated spectral Green's function that corresponds to either the voltage $(\mathbf{p} = \mathbf{e})$ or the current $(\mathbf{p} = \mathbf{h})$. The index i represents the order number of the rectangular waveguide mode ($\mathrm{TE}_{m,n}$ where $m, n = 0, 1, 2 \ldots, mn \neq 0$ or $\mathrm{TM}_{m,n}$ where $m, n = 1, 2, 3, \ldots$). The expressions for $\mathbf{e}_i$ and $\mathbf{h}_i$, the vector mode functions of electric and magnetic types for waveguides of rectangular cross sections, can be found in [1].

Introducing the rectangular waveguide Green's functions (7) into the expressions for MoM coefficients, (6) becomes

$$R_{PQ}(k,l) = \sum_i \widetilde{G}_{Pi}C_P(k,i)C_Q(l,i) \tag{8}$$

where

$$C_P(k,i) = \int_{S_k} \mathbf{f}_{Pk}(x,y)\mathbf{p}_i(x,y)\,\mathrm{d}x\,\mathrm{d}y. \tag{9}$$

It can be noticed from the above (8) that all MoM matrix coefficients are functions of only two different overlapping integrals. In particular, the overlapping integrals of the $\mathbf{e}$ and $\mathbf{h}$ vector mode functions with the vector basis functions. Having rectangular and/or triangular subsectional basis functions, these integrals can be computed analytically.

III. Efficient Evaluation of MoM Matrix

For efficient evaluation of the series in (8), the extraction of the quasi-static term of the spectral Green's functions is performed [2], [25], [26]. The main implication of this technique is

that the original series are separated into frequency-independent and frequency-dependent series. The frequency-independent series are evaluated only once for a given geometry and are, therefore, not recomputed for each new point in frequency. As for the frequency-dependent series, they are evaluated for each point in frequency, but due to the extraction of the quasi-static part, the convergence is enhanced considerably. As a result, an important saving in computational time for the analysis of multilayered media waveguide structures over a wide range of frequencies is achieved.

Dropping the P and Q indices, any MoM matrix coefficient in (8) can be written in the following general form:

$$R(k,l) = \sum_i \widetilde{G}_i C_{eh}(i,k) C_{eh}(i,l) \tag{10}$$

where C_{eh} is an overlapping integral of the $\mathbf{e}$ or $\mathbf{h}$ vector mode functions with the vector basis functions, and $\widetilde{G}_i$ is a voltage or current coefficient computed using equivalent transmission-line networks (spectral quantity). The first step in the procedure is to add and subtract to (10) the quasi-static term of the spectral-domain quantity $\widetilde{G}_i$ as follows:

$$R(k,l) = \sum_i \left(\widetilde{G}_i - \widetilde{G}_i^0\right) C_{eh}(i,k) C_{eh}(i,l) + R_0(k,l) \tag{11}$$

where $\widetilde{G}_i^0$ is the quasi-static part of $\widetilde{G}_i$, and we have defined

$$R_0(k,l) = \sum_i \widetilde{G}_i^0 C_{eh}(i,k) C_{eh}(i,l). \tag{12}$$

To obtain the quasi-static part, the case of modes infinitely below the cutoff has to be considered. The equivalent network for the quasi-static part is composed only of two semi-infinite transmission-line sections, above and below the exciting generator, i.e., the source point.

For the case of a HED as a source $(Q = E)$, the quasi-static part of the voltage coefficient is nonzero only for the basis functions belonging to that electric interface and is given by

$$R_0(k,l) = \mathrm{j} D^{\mathrm{TE}} R_0^{\mathrm{TE}}(k,l) + \frac{1}{\mathrm{j} D^{\mathrm{TM}}} R_0^{\mathrm{TM}}(k,l) \tag{13a}$$

with

$$R_0^{\mathrm{TE}}(k,l) = \sum_i \frac{1}{k_{\rho i}} C_{eh}^{\mathrm{TE}}(i,k) C_{eh}^{\mathrm{TE}}(i,l) \tag{13b}$$

$$R_0^{\mathrm{TM}}(k,l) = \sum_i k_{\rho i} C_{eh}^{\mathrm{TM}}(i,k) C_{eh}^{\mathrm{TM}}(i,l) \tag{13c}$$

$$D^{\mathrm{TE}} = \omega \mu_0 \frac{\mu_r^+ \mu_r^-}{\mu_r^+ + \mu_r^-} \tag{13d}$$

$$D^{\mathrm{TM}} = \omega \varepsilon_0 \left(\varepsilon_r^+ + \varepsilon_r^-\right) \tag{13e}$$

where C_{eh}^{TE} and C_{eh}^{TM} are the overlapping integrals between the basis functions of a given electric interface with the $\mathrm{TE}_{m,n}$ and $\mathrm{TM}_{m,n}$ modal sets, respectively, $k_{\rho i}$ is the transverse wavenumber of the ith mode, and the superscripts $+$ and $-$ are used to designate the dielectric parameters of the layers above and below the considered interface, respectively.

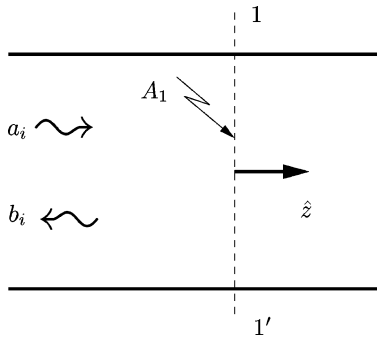

Fig. 3. Waveguide excitation.

Analogously, for an HMD as a source, $(Q = H)$, the quasi-static part of the current coefficient is nonzero only for the basis functions belonging to that magnetic interface and is given by

$$R_0(k,l) = \frac{1}{\mathrm{j} D^{\mathrm{TE}}} R_0^{\mathrm{TE}}(k,l) + \mathrm{j} D^{\mathrm{TM}} R_0^{\mathrm{TM}}(k,l) \tag{14a}$$

with

$$R_0^{\mathrm{TE}}(k,l) = \sum_i k_{\rho i} C_{eh}^{\mathrm{TE}}(i,k) C_{eh}^{\mathrm{TE}}(i,l) \tag{14b}$$

$$R_0^{\mathrm{TM}}(k,l) = \sum_i \frac{1}{k_{\rho i}} C_{eh}^{\mathrm{TM}}(i,k) C_{eh}^{\mathrm{TM}}(i,l). \tag{14c}$$

The interesting feature of (13b), (13c), (14b), and (14c) is that all the quantities depend only on geometry and are, therefore, frequency independent. Consequently, the series are computed only once for a given geometry and are not recomputed for each subsequent frequency point. Once they are summed up, the total quasi-static matrix coefficients are evaluated using of (13a) and (14a).

Substituting the quasi-static part in (11), the final MoM matrix coefficients are obtained, this time frequency dependent. It is important to note that since the quasi-static term is extracted, the resulting series will converge much faster than the original ones.

IV. Modal Excitation

Let the excitation of the waveguide be a source that produces a single mode of unit amplitude. This mode (usually the dominant mode) is denoted by the index i. The field transverse to the z-direction can be expressed in terms of the incident power wave a_i as

$$\mathbf{H}^{\mathrm{inc}} = \frac{a_i}{\sqrt{Z_i}} \mathbf{h}_i \tag{15}$$

where Z_i is the characteristic impedance and $\mathbf{h}_i$ is the magnetic field vector modal function of the considered mode.

Suppose that we want to compute the reflection coefficient in the reference plane $1\text{–}1'$ (Fig. 3). Let the aperture A_1 in that reference plane be discretized into a number of subsectional (rectangular and/or triangular) basis functions $\mathbf{f}_{Hk}$ for all indexes $k = 1, \ldots, N_H$ for which $S_k \subset A_1$.

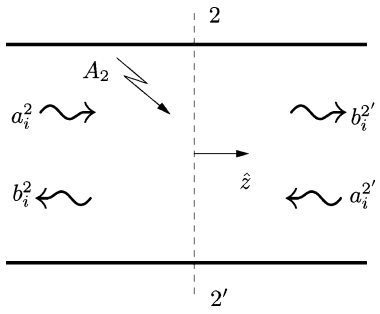

Fig. 4. Port for which the transmission coefficient is computed.

The excitation vector in the MoM system of equations (5) can then be expressed as follows:

$$\gamma_{Hk} = -2 \int_{S_k} \mathbf{H}^{\text{inc}} \cdot \mathbf{f}_{Hk} \, \mathrm{d}S \tag{16}$$

where the coefficient 2 comes from the "mirrored" magnetic field [27].

After having solved the system, we obtain, among the others, the unknown coefficients α_{Hk}, which are used to expand the magnetic current on the aperture A_1 in a given set of basis functions

$$\mathbf{J}_H = \sum_k \alpha_{Hk} \mathbf{f}_{Hk}. \tag{17}$$

The tangential electric field in the aperture, now that magnetic current is known, can be expressed as

$$\mathbf{E} = \hat{z} \times \mathbf{J}_H = \sum_k \alpha_{Hk} (\hat{z} \times \mathbf{f}_{Hk}). \tag{18}$$

On the other hand, this field can be represented with a mode expansion because it is also a field solution in the waveguide

$$\mathbf{E} = \sum_j (a_j + b_j) \sqrt{Z_j} \mathbf{e}_j. \tag{19}$$

By projecting the electric field onto the incident mode i over the aperture A_1, using the orthonormality of the modes, and taking into account (18), (19) becomes

$$b_i = -a_i - \frac{1}{\sqrt{Z_i}} \sum_k \alpha_{Hk} \int_{S_k} \mathbf{f}_{Hk} \cdot \mathbf{h}_i \, \mathrm{d}S \tag{20}$$

for all indices k for which $S_k \subset A_1$. The reflection coefficient on the aperture A_1 can now be expressed as

$$s_{11} = \frac{b_i}{a_i} = -1 - \frac{1}{a_i} \frac{1}{\sqrt{Z_i}} \sum_k \alpha_{Hk} \int_{S_k} \mathbf{f}_{Hk} \cdot \mathbf{h}_i \, \mathrm{d}S. \tag{21}$$

Suppose our structure has another port, defined at the reference plane $2 - 2'$, and we would like to compute the transmission coefficient between the two ports. Let the second port be attached to the right-hand side of the aperture A_2 at this reference plane (Fig. 4) and let the incident power wave that excites the port attached to the aperture A_1 (Fig. 3) be a_i^1. The transmission coefficient between the two ports is then defined as (see Fig. 4)

$$s_{21} = \frac{b_i^{2'}}{a_i^1} = \frac{a_i^2}{a_i^1}. \tag{22}$$

Taking into account that, by definition, the second port is perfectly matched $a_i^{2'} = b_i^2 = 0$ and following the same procedure as in (17)–(20), for the transmission coefficient, one obtains

$$s_{21} = -\frac{1}{a_i^1} \frac{1}{\sqrt{Z_i}} \sum_k \alpha_{Hk} \int_{S_k} \mathbf{f}_{Hk} \cdot \mathbf{h}_i \, \mathrm{d}S \tag{23}$$

for all indices k for which $S_k \subset A_2$.

Here, we presented numerical developments for a two-port waveguide structure, but they can be easily extended to a structure with several ports.

V. Efficient Numerical Treatment of Thick Irises

An iris of a finite thickness inside the rectangular waveguide can be solved using the theory presented in the previous sections as a cavity region with magnetic currents on its both interfaces. We will refer to this solution as the "full-wave cavity approach." This problem is equivalent to the problem of apertures of a finite thickness in printed multilayered antennas. However, recent results [23], [24] have shown that reasonably thick apertures can be treated as infinitely thin (Fig. 1). The aperture thickness appears only as a modification in the Green's functions of the problem, but otherwise the aperture is treated as a two-dimensional object. This technique reduces two times the number of unknowns on the aperture and, depending on how the correction term is computed, allows to treat the apertures of arbitrary cross sections. As shown in [23], the approximate treatment of thick apertures led to a perturbation term in the existing IE kernel. The IEs remain the same, save for the correction factor that is added to the Green's functions at the aperture interface

$$\overleftrightarrow{\mathbf{G}}_{HM} = \overleftrightarrow{\mathbf{G}}^{+}_{HM} + \overleftrightarrow{\mathbf{G}}^{-}_{HM} + 2\overleftrightarrow{\mathbf{G}}^{\Delta}_{HM} \tag{24}$$

where the superscripts $+$ and $-$ designate the region above and below the thick aperture.

The possibility of not being forced to consider the volume defining the thick aperture/iris as a new waveguide region is the keystone of the efficient procedure presented in this paper. However, to implement a particular computational algorithm, we shall need a fast and accurate way of evaluation of the Green's function correction term $\overleftrightarrow{\mathbf{G}}^{\Delta}_{HM}$.

The correction term that accounts for a thick iris is given by [23], [24]

$$\overleftrightarrow{\mathbf{G}}^{\Delta}_{HM} = \overleftrightarrow{\mathbf{G}}^{=}_{HM} - \overleftrightarrow{\mathbf{G}}^{\times}_{HM} \tag{25}$$

where $\overleftrightarrow{\mathbf{G}}^{=}_{HM}$ is the Green's function of the thick iris region when both source and observer points are on the same iris interface, and $\overleftrightarrow{\mathbf{G}}^{\times}_{HM}$ is the same Green's function when they are on the opposite iris interfaces.

One approach in efficient computing of the correction term is to neglect the iris' walls and use a parallel-plate equivalent

waveguide ("PEW" approach). A second one, more accurate, is to use the true Green's functions of the thick iris cavity ("TIC" approach).

In the "PEW" approach, the thick iris correction term is computed in the way presented in [23] and [24]. There, correction terms for the potential Green's functions of the thick iris are approximated using the parallel-plate Green's function. This approximation will remain valid for all shapes of the thick irises as long as the iris' thickness is sufficiently small compared to its minimal lateral dimensions [23].

The correction terms for vector and scalar potential Green's functions $\overleftrightarrow{\mathbf{G}}_F^{\Delta} = \overleftrightarrow{\mathbf{G}}_F^{=} - \overleftrightarrow{\mathbf{G}}_F^{\times}$ and $G_V^{\Delta} = G_V^{=} - G_V^{\times}$, respectively, are obtained applying the zeroth-order inverse Sommerfeld transformation $\mathcal{S}_0$ to the parallel-plate spectral-domain Green's function [24], [28]

$$G_{Fxx}^{\Delta} = G_{Fyy}^{\Delta} = \frac{\varepsilon}{2\pi}\mathcal{S}_0\left[\frac{1}{k_z}\tan\frac{k_z t}{2}\right] \tag{26a}$$

$$G_W^{\Delta} = \frac{1}{2\pi\mu}\mathcal{S}_0\left[\frac{1}{k_z}\tan\frac{k_z t}{2}\right] \tag{26b}$$

where t is the thickness of the considered iris and k_z is the propagation constant inside the iris in the z-direction. The difference with respect to the approach presented in [23] and [24] is in the fact that the correction terms are not added in the level of the spectral-domain Green's functions, but on the MoM coefficient level. The MoM coefficients of the iris are computed as if it were infinitely thin using the theory presented in the previous sections. The correction terms in MoM coefficients are then computed using the mixed potential integral equation (MPIE) and the potential Green's functions (26) and added to already computed MoM coefficients.

In the "TIC" approach, the Green's function correction term for field Green's functions is expressed as a sum of modes (rectangular waveguide modes), obtaining in this way a consistent IE approach that always uses (for closed regions) the modal field Green's functions. In this approach, the correction term will necessarily depend on the thick iris cross section.

If we consider the rectangular iris, the Green's function can be written as

$$\overleftrightarrow{\mathbf{G}}_{HM} = \sum_i \widetilde{G}_{Hi}(z,z')\mathbf{h}_i(x,y)\mathbf{h}_i(x',y') \tag{27}$$

where $\widetilde{G}_{Hi}(z,z')$ is the current evaluated at the coordinate z along the equivalent transmission-line network, when the exciting generator is set to one and placed at the coordinate z' in the direction of propagation, and $\mathbf{h}_i$ is the vector mode of magnetic type for waveguides with rectangular cross sections.

Taking into account (25) and (27), the Green's function correction term can be expressed as

$$\overleftrightarrow{\mathbf{G}}_{HM}^{\Delta} = \sum_i \widetilde{G}_{Hi}^{\Delta}\mathbf{h}_i(x,y)\mathbf{h}_i(x',y') \tag{28}$$

where

$$\widetilde{G}_{Hi}^{\Delta} = \frac{\mathrm{j}}{Z_{\mathrm{c}_i}}\tan\left(\frac{k_{z_i}t}{2}\right). \tag{29}$$

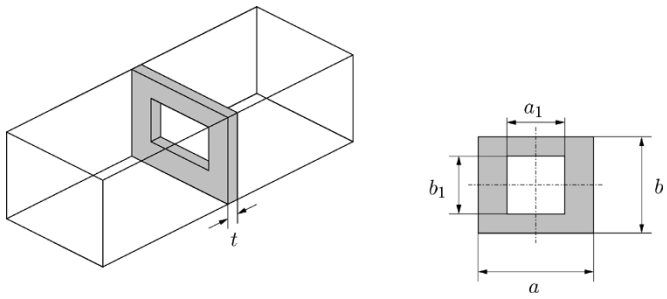

Fig. 5. Thick iris inside rectangular waveguide: $a = 22.86, b = 10.16, a_1 = 11.43$, $b_1 = 5.08$, and t is variable iris thickness. All dimensions given in millimeters.

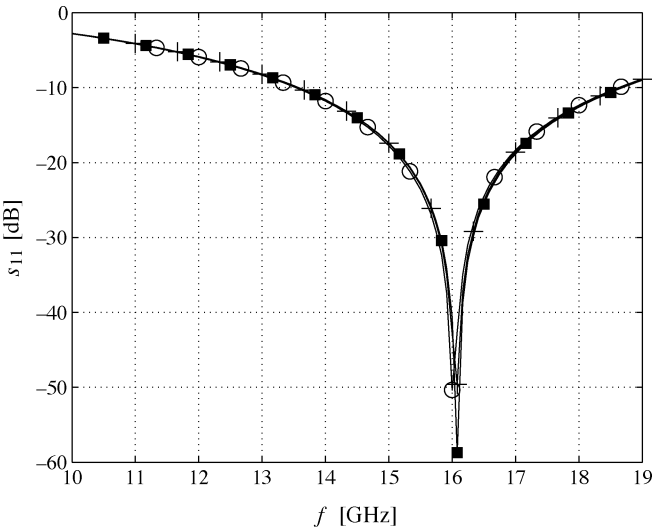

Fig. 6. Reflection coefficient for iris thickness $t = 0.1\,\mathrm{mm} = \lambda/200$: "PEW" ($\circ$), "TIC" ($+$), full-wave cavity approach ($\blacksquare$).

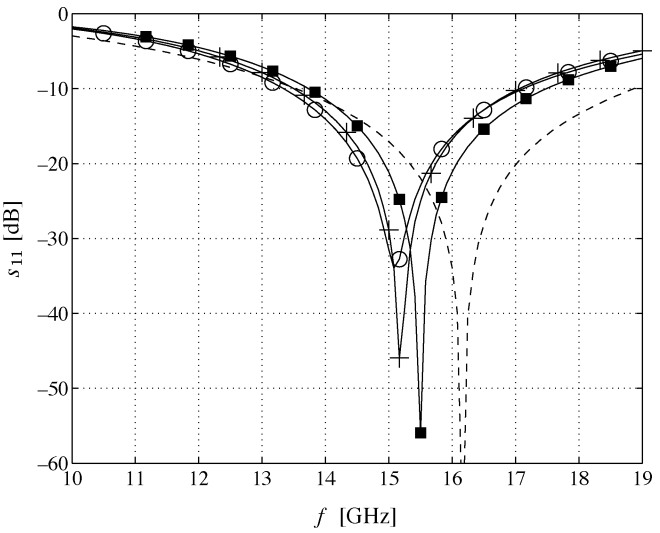

Fig. 7. Reflection coefficient for iris thickness $t = 1\,\mathrm{mm} = \lambda/20$: "PEW" ($\circ$), "TIC" ($+$), full-wave cavity approach ($\blacksquare$), and zero thickness iris (dashed line).

VI. Numerical Results for Thick Iris Problems

The first test-structure simulated is a simple rectangular waveguide WR90 with a thick rectangular iris of dimensions $a_1 = a/2$ and $b_1 = b/2$ placed at the center of the waveguide's cross section (Fig. 5). Simulations have been performed for iris thicknesses up to 1 mm ($\lambda/20$ at the center frequency). Figs. 6 and 7 show results for two thicknesses: 0.1 and 1 mm.

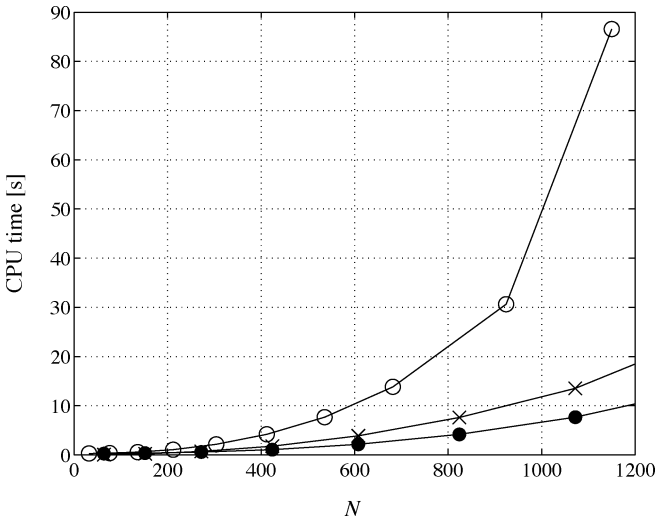

Fig. 8. CPU time versus number of unknowns for a problem from Fig. 5 solved using the full-wave cavity approach ($\circ$), the "PEW" ($\bullet$), and the "TIC" approach ($\times$) with the same mesh density.

In both figures, the reflection coefficients shown are simulated using the "PEW" approach ($\circ$), the "TIC" approach ($+$), the full-wave cavity approach ($\blacksquare$), and supposing that the iris is infinitely thin (dashed line). In the full-wave approach, the simulations were done with 5000 modes used in computation of the quasi-static terms (frequency independent) and 1000 modes for computation of dynamic terms (frequency dependent). In the "PEW" approximate approach, the correction factor was computed taking into account the dimensions of the rectangular iris cross section. The quasi-static term was not extracted. Number of modes used for computing dynamic terms was 1000. The results reached the numerical convergence since we obtain the same response when the number of modes is doubled and even three times bigger. The almost perfect matching of the "PEW" and "TIC" approaches with the full-wave cavity approach taken as a reference can be observed up to iris thicknesses of $t = 0.1$ mm $= \lambda/200$ at the center frequency $f = 15$ GHz. Above this thickness, the approximate models predict the scattering parameters less accurately, but still better than the zero thickness approach (dashed lines in Fig. 7).

Fig. 8 shows the CPU time versus the number of unknowns for the problem from Fig. 5 solved using the full-wave approach ($\circ$), the "PEW" approach ($\bullet$), and the "TIC" approach ($\times$) on a PC with 2.4 GHz and 512 MB of RAM. As can be seen from this figure, the problem solved using the approximate approaches with the same mesh density as in the full-wave cavity problem will have a twice smaller number of unknowns (the thick iris is accounted for as an infinitely thin iris with the correction factor in the Green's function) and the corresponding CPU time will be significantly smaller. Note that, in Fig. 8, the number of unknowns N corresponds to the problem solved using the full-wave approach.

A second example is a strip-to-slot transition module (Fig. 9), which has been presented in [20] as a benchmark for the GSM method. For the case of a zero-thickness slot, our IE approach shows excellent agreement (Fig. 10) with the results of [20]. This is a good validation case for our technique. In addition, finite thickness slots/irises can be analyzed with only a small

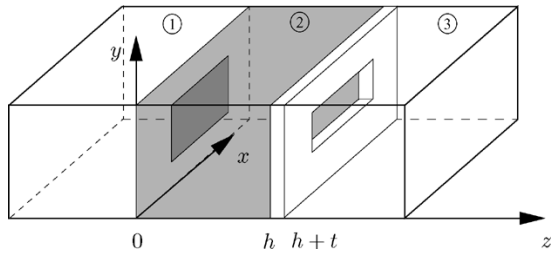

Fig. 9. Geometry of a rectangular waveguide-based strip-to-slot transition module. All dimensions are given in millimeters [20]. Waveguide WR90: $a = 22.86$, $b = 10.16$. Strip: $a_1 = 10.4$, $b_1 = 9.0$. Slot: $a_2 = 10.4$, $b_2 = 0.2$. Dielectrics: $\varepsilon_1 = 1.0, \varepsilon_2 = 6.0, \varepsilon_3 = 1.0$, $h = 0.381$, t—variable slot/iris thickness.

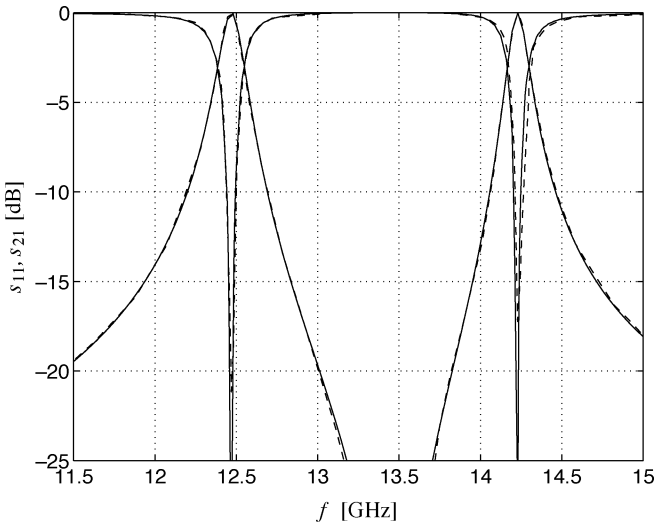

Fig. 10. Magnitude of the reflection s_{11} and transmission s_{21} coefficients against frequency for a resonant strip-to-slot transition. Numerical results (solid lines) are compared with results obtained using GSM in conjunction with MoM taken from [20] (dashed lines). Slot thickness $t = 0$ mm.

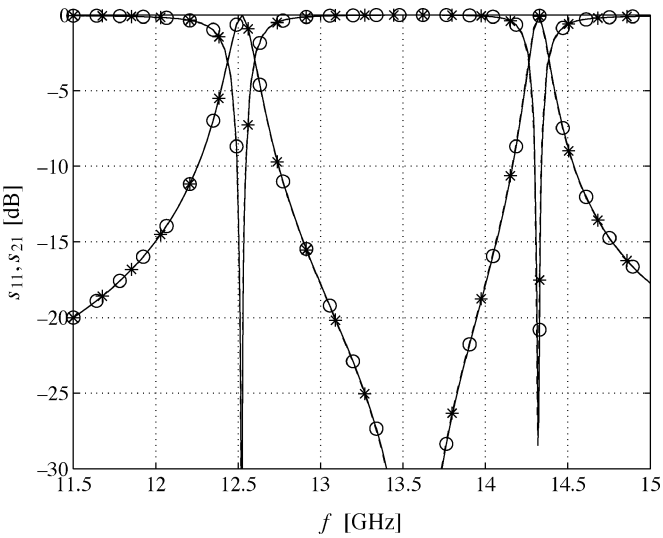

Fig. 11. Magnitude of the reflection s_{11} and transmission s_{21} coefficients against frequency for a resonant strip-to-slot transition. Approximate approach using "TIC" method (solid lines with $\circ$) are compared with results obtained using full-wave approach (dashed lines with $*$). Iris thickness $t = 0.1$ mm.

overhead in the computational effort. Figs. 11 and 12, where we compare the full-wave approach with the approximate "TIC"

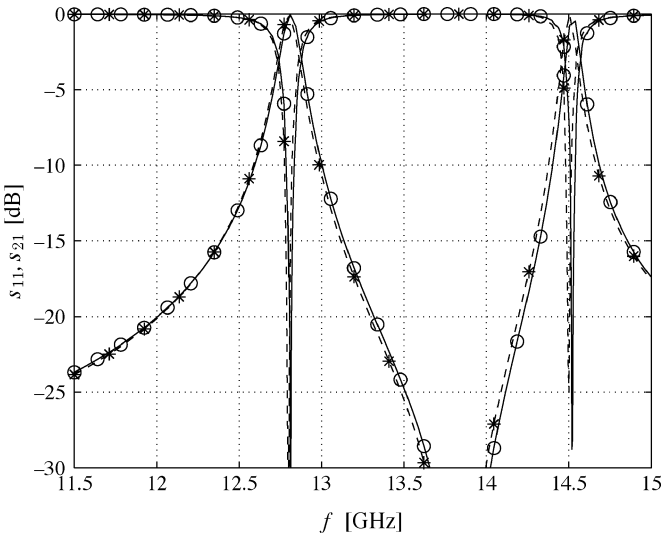

Fig. 12. Magnitude of the reflection s_{11} and transmission s_{21} coefficients against frequency for a resonant strip-to-slot transition. Approximate approach using "TIC" method (solid lines with $\circ$) are compared with results obtained using full-wave approach (dashed lines with $*$). Iris thickness $t = 1$ mm.

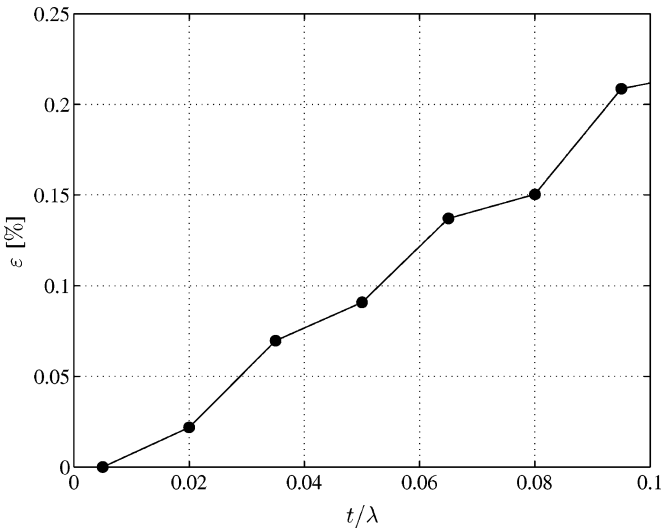

Fig. 13. Relative error in predicted resonance frequency as a function of the iris thickness t. The wavelength is computed for $f = 15$ GHz.

strategy, give results for slot thicknesses $t = 0.1$ mm and $t = 1$ mm. Agreement is excellent with only a small frequency shift observed for $t = 1$ mm. We have performed a systematic check of the error introduced in the resonant frequency by the "TIC" approach. Fig. 13 shows that this error increases linearly with the iris thickness and remains acceptable (0.2%) for thicknesses up to 0.1λ. Finally, we have tried to characterize the overall error generated in typical scattering parameters over the whole frequency band. To this end, we have defined a root mean square (rms) error computed as

$$\varepsilon_{\mathrm{rms}} = \sum_{i=1}^{N} \sqrt{\frac{|x_i - y_i|^2}{|y_i|^2}} \tag{30}$$

where y_i is a scattering parameter computed at different frequency points i using the full-wave approach and x_i is the same scattering parameter computed using the approximate "TIC"

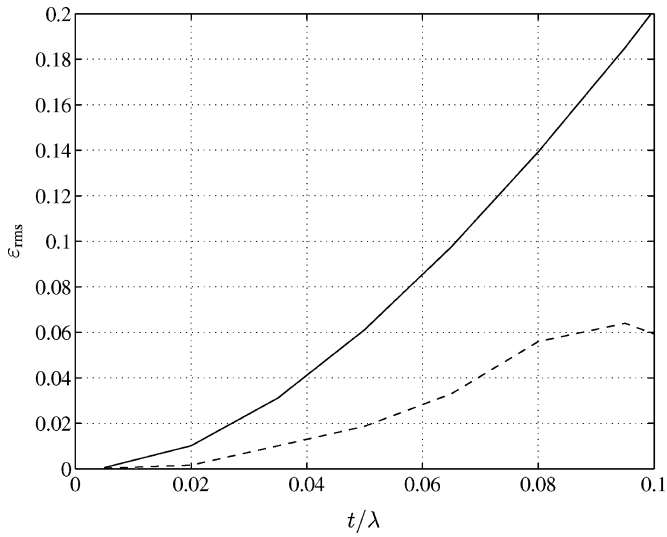

Fig. 14. rms error in the transmission coefficient as a function of the iris thickness t (solid line). The same error after the frequency shift in predicted resonance frequencies has been taken into account (dashed line). The wavelength is computed for $f = 15$ GHz.

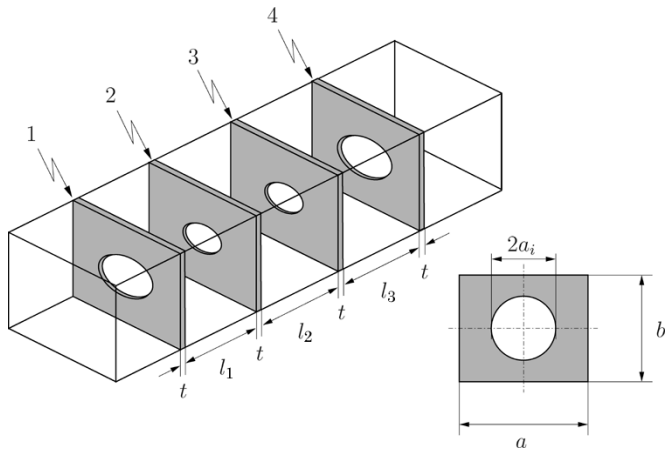

Fig. 15. Circular iris coupled rectangular waveguide three-resonator filter. Filter dimensions are in millimeters [13]: $a = 15.8$, $b = 7.9$, $t = 0.218$, $a_1 = 2.577$, $a_2 = 1.142$, $a_3 = 1.125$, $a_4 = 2.592$, $l_1 = 12.499$, $l_2 = 12.819$, $l_3 = 12.461$.

approach. Fig. 14 shows the rms error before and after having accounted for the resonance frequency correction. After the correction, the rms error in the whole frequency band remains below 6% for thicknesses up to 0.1λ.

Finally, we have simulated the circular iris coupled resonator filter shown in Fig. 15 [13]. For this problem, the "PEW" approach did not provide accurate enough results and the Green's function correction factor, calculated using the "TIC" approach, has been preferred. For the correction factors, rectangular waveguides of the cross sections that circumscribe the cross sections of the circular irises are used. As can be seen from Fig. 16, the results for the insertion loss simulated using our approach are in excellent agreement with the measured values taken from [13], which demonstrates the precision of our technique. The irises in this practical example are rather thin, being a hundredth of the operating wavelength. However, neglecting this thickness when simulating the structure would lead to erroneous results (dashed line in the same figure).

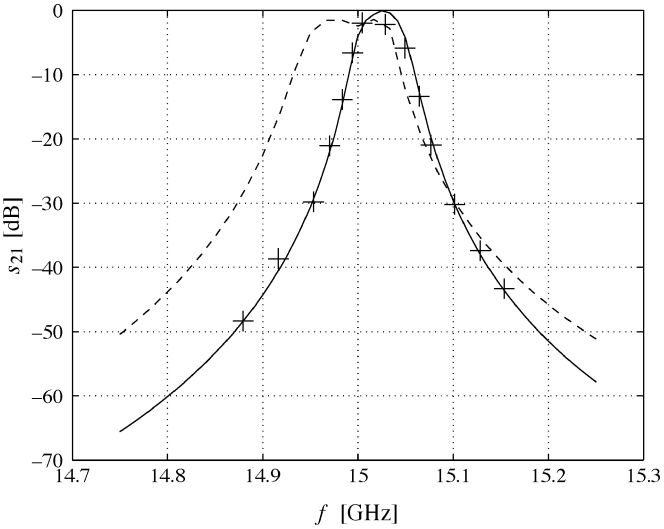

Fig. 16. Insertion loss of the iris coupled resonant filter: simulation using the "TIC" approach (solid line) and measured values (+) taken from [13]. The dashed line represents the simulation with infinitely thin irises.

VII. Conclusion

In this paper, we have surveyed the IE models for finite thickness irises and applied them to several rectangular waveguide discontinuities and filter configurations including irises. It is obvious that above a certain thickness, only a rigorous model treating the irises themselves as cavities can provide accurate results. However, for moderate thicknesses (up to 0.1λ), reasonable accuracy can be obtained by combining a recently introduced approximate model for finite thickness slots with a classical integral formulation of waveguide discontinuities. The proposed technique then reduces by a factor of 2 the number of unknowns in every iris and, thus, includes the effect of irises' thickness with no increase in the computational complexity associated to zero-thickness irises. The key point of the approach is to include the thickness as an analytical correction in the Green's function that must be used when solving irises with the equivalence principle. Two practical formulations of this correction factor have been discussed and implemented with excellent results. The roughest and simplest one (the "PEW" approach) can be applied to irises of any shape, but they must be large and not very thick because the coupling phenomena corresponding to the irises' lateral walls are neglected. If this assumption cannot be made, an alternative way of computing the Green's function correction (the "TIC" approach) is proposed, which is valid for shapes where the waveguide modes have an analytical expression. This second alternative represents only a slight overhead in computer time and, hence, it is always preferable to the zero thickness approach. Moreover, our approach is very accurate when compared with a full-wave approach for thicknesses of the order of several hundredths of a wavelength. For these thicknesses, frequently encountered in current technologies, the zero-thickness model does not provide the accuracy requested in many modern applications.

References

[1] N. Marcuvitz, *Waveguide Handbook*. New York: McGraw-Hill, 1951.
[2] L. Lewin, *Theory of Waveguides*. London, U.K.: Butterworths, 1975.
[3] R. E. Collin, *Field Theory of Guided Waves*. New York: McGraw-Hill, 1960.
[4] G. Matthaei, L. Young, and E. M. T. Jones, *Microwave Filters, Impedance-Matching Networks, and Coupling Structures*. New York: McGraw-Hill, 1964.
[5] R. J. Luebbers and B. A. Munk, "Analysis of thick rectangular waveguide windows with finite conductivity," *IEEE Trans. Microw. Theory Tech.*, vol. MTT-21, no. 7, pp. 461–468, Jul. 1973.
[6] R. Levy, "Improved single and multiaperture waveguide coupling theory, including explanation of mutual interactions," *IEEE Trans. Microw. Theory Tech.*, vol. MTT-28, no. 4, pp. 331–338, Apr. 1980.
[7] A. Jennings and R. L. Gray, "Extension of Levy's large-aperture design formulas to the design of circular irises in coupled-resonator waveguide filters," *IEEE Trans. Microw. Theory Tech.*, vol. MTT-23, no. 11, pp. 1489–1493, Nov. 1984.
[8] P. J. B. Clarricoats and K. R. Slinn, "Numerical solution of waveguide-discontinuities," *Proc. Inst. Elect. Eng.*, pt. H, vol. 114, pp. 878–886, Jul. 1967.
[9] A. Wexler, "Solution of waveguide discontinuities by modal analysis," *IEEE Trans. Microw. Theory Tech.*, vol. MTT-15, no. 9, pp. 508–517, Sep. 1967.
[10] H. Patzelt and F. Arndt, "Double-plane steps in rectangular waveguide and their application for transformers, irises and filters," *IEEE Trans. Microw. Theory Tech.*, vol. MTT-29, no. 5, pp. 771–777, May 1982.
[11] M. S. Navarro, T. E. Rozzi, and Y. Z. Lo, "Propagation in a rectangular waveguide periodically loaded with resonant irises," *IEEE Trans. Microw. Theory Tech.*, vol. MTT-28, no. 8, pp. 857–865, Aug. 1980.
[12] F. Arndt, J. Bornemann, D. Heckmann, C. Piontek, H. Semmerow, and H. Schueler, "Modal-S-matrix method for the optimum design of inductively direct-coupled cavity filters," *Proc. Inst. Elect. Eng.*, pt. H, vol. 133, pp. 341–350, 1986.
[13] U. Papziner and F. Arndt, "Field theoretical computer-aided design of rectangular and circular iris coupled rectangular of circular waveguide cavity filters," *IEEE Trans. Microw. Theory Tech.*, vol. 41, no. 3, pp. 462–470, Mar. 1993.
[14] M. Guglielmi, G. Gheri, M. Calamia, and G. Pelosi, "Rigorous multimode network representation of inductive steps," *IEEE Trans. Microw. Theory Tech.*, vol. 42, no. 2, pp. 317–326, Feb. 1994.
[15] L. Valor and J. Zapata, "Efficient finite element analysis of waveguides with lossy inhomogeneous anisotropic materials characterized by arbitrary permittivity and permeability tensors," *IEEE Trans. Microw. Theory Tech.*, vol. 43, no. 10, pp. 2452–2459, Oct. 1995.
[16] J. Rubio, J. Arroyo, and J. Zapata, "SFELP—An efficient methodology for microwave circuit analysis," *IEEE Trans. Microw. Theory Tech.*, vol. 49, no. 3, pp. 509–516, Mar. 2001.
[17] R. Beyer and F. Arndt, "Efficient modal analysis of waveguide filters including the orthogonal mode coupling elements by an MM/FE method," *IEEE Microw. Guided Wave Lett.*, vol. 5, no. 1, pp. 9–11, Jan. 1995.
[18] F. Arndt, J. Brandt, V. Catina, J. Ritter, I. Rullhusen, J. Dauelsberg, U. Hilgefort, and W. Wessel, "Fast CAD and optimization of waveguide components and aperture antennas by hybrid MM/FE/MoM/FD methods—State-of-the-art and recent advances," *IEEE Trans. Microw. Theory Tech.*, vol. 52, no. 1, pp. 292–305, Jan. 2004.
[19] A. I. Khalil, A. B. Yakovlev, and M. B. Steer, "Efficient method-of-moments formulation for the modeling of planar conductive layers in a shielded guided-wave structure," *IEEE Trans. Microw. Theory Tech.*, vol. 47, no. 9, pp. 1730–1736, Sep. 1999.
[20] A. B. Yakovlev, A. I. Khalil, C. W. Hicks, A. Mortazawi, and M. B. Steer, "The generalized scattering matrix of closely spaced strip and slot layers in waveguide," *IEEE Trans. Microw. Theory Tech.*, vol. 48, no. 1, pp. 126–137, Jan. 2000.
[21] T. Shibata and T. Itoh, "Generalized-scattering-matrix modeling of waveguide circuits using FDTD field simulations," *IEEE Trans. Microw. Theory Tech.*, vol. 46, no. 11, pp. 1742–1751, Nov. 1998.
[22] H. Auda and R. F. Harrington, "A moment solution for waveguide junction problems," *IEEE Trans. Microw. Theory Tech.*, vol. MTT-31, no. 7, pp. 515–520, Jul. 1983.
[23] J. R. Mosig, "Scattering by arbitrarily shaped slots in thick conducting screens: An approximate solution," *IEEE Trans. Antennas Propag.*, vol. 52, no. 8, pp. 2109–2117, Aug. 2004.
[24] I. Stevanović and J. R. Mosig, "Efficient electromagnetic analysis of line-fed aperture antennas in thick conducting screens," *IEEE Trans. Antennas Propag.*, vol. 52, no. 11, pp. 2896–2903, Nov. 2004.
[25] C. J. Railton and S. A. Meade, "Fast rigorous analysis of shielded planar filters," *IEEE Trans. Microw. Theory Tech.*, vol. 40, no. 5, pp. 978–985, May 1992.

[26] G. V. Eleftheriades, J. R. Mosig, and M. Guglielmi, "A fast integral equation technique for shielded planar circuits defined on nonuniform meshes," *IEEE Trans. Microw. Theory Tech.*, vol. 44, no. 12, pp. 2293–2296, Dec. 1996.
[27] J. Van Bladel, *Electromagnetic Fields*. New York: McGraw-Hill, 1964.
[28] J. R. Mosig, "Integral-equation technique," in *Numerical Techniques for Microwave and Millimeter-Wave Passive Structures*, T. Itoh, Ed. New York: Wiley, 1989, ch. 3, pp. 133–213.

Ivica Stevanović (S'03–M'06) was born in Kruševac, Serbia, in 1976. He received the Dipl.Ing. degree in electrical engineering from the University of Belgrade, Belgrade, Serbia, in 2000, and the Ph.D. degree in electrical engineering from the Ecole Polytechnique Fédérale de Lausanne (EPFL), Lausanne, Switzerland, in 2005.

From 1998 to 2000, he was a Student Assistant with the Laboratory of Electronics, School of Electrical Engineering (ETF), University of Belgrade. In Summer 2000, he was a SURF Research Fellow with the Laser Interferometer Gravitational Wave Observatory (LIGO), California Institute of Technology (Caltech), Pasadena. In November 2000, he joined the Laboratory of Electromagnetics and Acoustics (LEMA), EPFL, where he is currently a Research and Teaching Assistant. He is involved in several projects for the European Space Agency (ESA), Swiss Federal Office of Communications (OFCOM), and the European Networks of Excellence on metamaterials (METAMORPHOSE) and antennas (ACE).

Dr. Stevanović was the recipient of a scholarship presented by the Serbian Ministry of Education (1997–2000) and a research fellowship (SURF) presented by Caltech.

Pedro Crespo-Valero was born in Antas (Almería), Spain, in 1976. He received the Ingeniero de Telecomunicación degree from the Universidad Politécnica de Madrid (UPM), Madrid, Spain, in 2001, and is currently working toward the Ph.D. degree at the Ecole Polytechnique Fédérale de Lausanne (EPFL), Lausanne, Switzerland.

In February 2002, he joined the Laboratory of Electromagnetics and Acoustics (LEMA), EPFL, where he is a Research and Teaching Assistant. He is involved in several projects with the European Space Agency (ESA) and other European universities and industries. His research interests include the computer-aided design (CAD) of microwave passive devices and circuits.

Mr. Crespo-Valero is a member of Colegio Mayor Diego de Covarrubias, Universidad Complutense de Madrid (UCM), Madrid, Spain.

Juan R. Mosig (S'76–M'87–SM'94–F'99) was born in Cadiz, Spain. He received the Electrical Engineer degree from the Universidad Politecnica de Madrid, Madrid, Spain, in 1973, and the Ph.D. degree from the Ecole Polytechnique Fédérale de Lausanne (EPFL), Lausanne, Switzerland, in 1983.

In 1976, he joined the Laboratory of Electromagnetics and Acoustics, EPFL. Since 1991, he has been a Professor with EPFL and since 2000, he has been the Head of the Laboratory of Electromagnetics and Acoustics (LEMA), EPFL. In 1984, he was a Visiting Research Associate with the Rochester Institute of Technology, Rochester, NY, and Syracuse University, Syracuse, NY. He has also held scientific appointments with the University of Rennes, Rennes, France, the University of Nice, Nice, France, the Technical University of Denmark, Lyngby, Denmark, and the University of Colorado at Boulder. He is co-organizer and lecturer of yearly short courses in numerical electromagnetics in both Europe and the U.S. He is also responsible for several research projects of the European Space Agency (ESA). He has authored four chapters in books on microstrip antennas and circuits and over 100 reviewed papers. His research interests include electromagnetic theory, numerical methods, and planar antennas.

Dr. Mosig is a member of the Swiss Federal Commission for Space Applications, the chairman of the European COST Project on Antennas (2003–2006), and a member of the Executive Board of the European Network of Excellence ACE (2004–2005).